

Crossover to negative dielectric response in the low-frequency spectra of metallic polymersKwanghee Lee¹ and A. J. Heeger²¹*Department of Physics, Pusan National University, Pusan 609-735, Korea*²*Institute for Polymers and Organic Solids, University of California, Santa Barbara, California 93106*

(Received 10 March 2003; published 1 July 2003)

We report high-precision reflectance, $R(\omega)$, measurements on films of conducting polypyrrole oriented by tensile drawing. The results obtained from Kramers-Kronig analysis of $R(\omega)$ demonstrate that the optical conductivity, $\sigma(\omega)$, becomes frequency-independent below approximately 250 cm^{-1} and that there is a zero crossing in the dielectric function, $\varepsilon(\omega)$, to negative values below 20 cm^{-1} . Since $\sigma(\omega)$ extrapolates to the dc value and since $\varepsilon(\omega)$ is in excellent agreement with the data obtained from terahertz and microwave measurements, the controversy in the dielectric response of the metal physics of conducting polymers is finally resolved.

DOI: 10.1103/PhysRevB.68.035201

PACS number(s): 71.20.Rv, 72.15.Rn, 72.80.Le, 78.66.Qn

I. INTRODUCTION

Highly conducting (“metallic”) polymers are in use in applications ranging from electrodes in capacitors to injection layers in “plastic electronic devices.”¹ Nevertheless, the natures of the metallic state and the metal-insulator (M-I) transition remain controversial and are not fully understood.^{2,3} The electrodynamic response at low frequencies is the central unresolved issue.⁴ While the dielectric function $\varepsilon(\omega)$ inferred from infrared reflectance measurements^{5–9} extrapolated to a positive value in the far infrared, direct measurements of the dielectric function in the microwave^{10,11} and terahertz ranges^{12,13} revealed $\varepsilon < 0$. The contradictory results have been a subject of considerable discussion.

The complicated transport properties of “metallic” polymers have been discussed as originating from the complex morphology of the materials, i.e., originating from structural inhomogeneities in the nanolength scale (the inhomogeneous or “metallic island” limit).^{3,14,15} Although it is true that such structural inhomogeneities dominated the physics of early materials, progress during the 1990s resulted in methods of processing high-quality uniform films from solution and enabled subsequent tensile drawing of such films to chain-extended and -oriented materials. The ability to process “metallic” polymers from solution has significantly improved the quality of the materials to a level at which the electronic length scales are larger than the size of the residual inhomogeneities.^{2,4,6} Although “homogeneous,” these materials are at best partially crystalline^{16,17} and are therefore disordered. Indeed, attempts to analyze the transport properties of the improved systems within the framework of conventional localization theory^{2,18,19} have been quite successful; “metallic” polymers can be quantitatively described as disordered metals near the metal-insulator transition.² Moreover, high magnetic fields and high pressure can be used to fine-tune the M-I transition; the use of high magnetic fields enabled studies of the crossover from metal to insulator,² and the use of high pressure enabled studies of the crossover from insulator to metal.²

Infrared (IR) reflectance measurements^{4–9} have played an important role in clarifying the metal physics of conducting

polymers. Infrared measurements and dc measurements probe different aspects of electronic transport; whereas dc transport experiments measure the bulk conductivity in which the transport is limited by the slowest processes, optical measurements probe the charge dynamics over a characteristic length scale of $L_\omega = (D/\omega)^{1/2}$ (D is the electron diffusion coefficient). It is gratifying, therefore, that Kramers-Kronig analysis of the IR reflectance data yields values for the optical conductivity $\sigma(\omega)$ that extrapolate directly to the measured dc values.^{4–6} Moreover, the functional dependencies of $\varepsilon(\omega)$ and $\sigma(\omega)$ can be quantitatively understood in terms of the conventional Drude model modified by the effect of weak localization,^{4,5} indicative of a homogeneous but disordered material over a wide range of length scales.

Dielectric measurements also provide information on the metallic state of conducting polymers. Direct measurements of the dielectric function in the far IR and at microwave frequencies^{10–13} probe the intraband excitations near the Fermi level. Studies of the dielectric loss (dielectric relaxation) in conducting polymers, employing ac-impedance measurements²⁰ or thermally stimulated depolarization current spectroscopy,²¹ probe localized charge motion (e.g., polarons) within nanometer-scale regions.

In spite of the robust evidence for the disorder-induced M-I transition as inferred from the transport² and optical measurements,^{4–6} the metallic state of conducting polymers remains a subject of controversy. Although several independent optical measurements^{6–9} demonstrated $\varepsilon(\omega) > 0$ for $\omega \geq 50\text{ cm}^{-1}$, as predicted by the “localization-modified Drude (LMD) model,”^{4,5} recent data from Martens *et al.*^{12,13} show $\varepsilon(\omega) < 0$ in the range of 8–600 GHz ($\approx 0.3\text{--}20\text{ cm}^{-1}$) in agreement with earlier microwave ($\approx 6.5\text{ GHz}$; 0.2 cm^{-1}) results.^{10,11} Some IR studies^{14,15} have even reported a zero crossing to $\varepsilon_1 < 0$ at much higher frequencies around $\sim 250\text{ cm}^{-1}$.

We report $\sigma(\omega)$ and $\varepsilon(\omega)$ obtained from Kramers-Kronig analysis of polarized reflectance measurements on high-quality, stretch-oriented films of metallic polypyrrole (PPy) doped with PF₆. Since tensile drawing improves the physical properties of the films by chain extension and chain alignment, we expect that high-precision reflectance measure-

ments carried out on such materials will resolve the controversy concerning the dielectric response. The results unambiguously demonstrate a crossover in the optical response with a zero crossing in $\epsilon(\omega)$ at approximately 20 cm^{-1} , i.e., at the boundary between the infrared⁵⁻⁹ and microwave (terahertz) regimes.^{12,13} These results fully reconcile the seemingly contradictory data described in the previous paragraphs and resolve the controversy.

II. DETAILS OF THE EXPERIMENTS

High-quality, metallic PPy-PF₆ films were prepared by galvanostatic (electrochemical) polymerization.²² The as-grown films (dc conductivity $\sigma_{dc} \approx 350 \text{ S/cm}$) were then tensile-drawn to a draw ratio $\ell/\ell_0 \approx 1.5$, resulting in a substantial increase in σ_{dc} along the draw axis, $\sigma_{dc\parallel} \approx 800 \text{ S/cm}$ at 300 K and a significant anisotropy, $\sigma_{dc\parallel}/\sigma_{dc\perp} \approx 4.6$ with $\sigma_{dc\perp} \approx 175 \text{ S/cm}$. Complete characterization by transport and x-ray-diffraction measurements was carried out to ensure sample quality before and after the tensile drawing. The resulting samples exhibited high-quality metallic properties.²² Scanning electron microscope inspection reveals surfaces with excellent optical quality even after the mechanical elongation. Reflectance, $R(\omega)$, was measured at room temperature with polarization parallel and perpendicular to the draw direction (using two different spectrometers) over the spectral range from 50 to 50 000 cm^{-1} (0.006–6 eV) as described previously.^{5,6}

The optical conductivity and dielectric function, as determined by Kramers-Kronig (K-K) analysis of the reflectance, are very sensitive to the details of $R(\omega)$, especially in the far IR. In particular, since we are concerned with the low-frequency region for establishing the details of the metal physics, accurate extrapolation beyond the lower measurement limit (typically by the Hagen-Rubens relation) is crucial.²³ Therefore, we extended the measured frequency range down to 8 cm^{-1} and enhanced the accuracy by utilizing higher sensitivity far-IR spectrometers; for the nonoriented sample, $R(\omega)$ was extended to $8 \leq \omega \leq 13 \text{ cm}^{-1}$ using a submillimeter spectrometer and to $20 \leq \omega \leq 100 \text{ cm}^{-1}$ using an interferometer (Bruker, 113v) equipped with a He-cooled Si bolometer. The results demonstrate the accuracy and precision of the $R(\omega)$ measurements and justify the low-frequency extrapolation using the Hagen-Rubens relation.

III. RESULTS AND DISCUSSION

Figure 1 shows $R(\omega)$ of partially oriented PPy-PF₆ measured with polarization parallel and perpendicular to the draw direction. Data from an as-grown sample (nonoriented) are shown for comparison. $R(\omega)$ of the as-grown sample is typical of the highest-quality PPy-PF₆ with a well-defined plasma frequency as indicated by the minimum in $R(\omega)$ at approximately $1.5 \times 10^4 \text{ cm}^{-1}$ and high $R(\omega)$ in the far IR. The uniaxial orientation induces anisotropy and causes an improvement in the physical properties of the films; for parallel polarization, $R(\omega)$ is enhanced throughout the IR. For perpendicular polarization, $R(\omega)$ remains below that of the

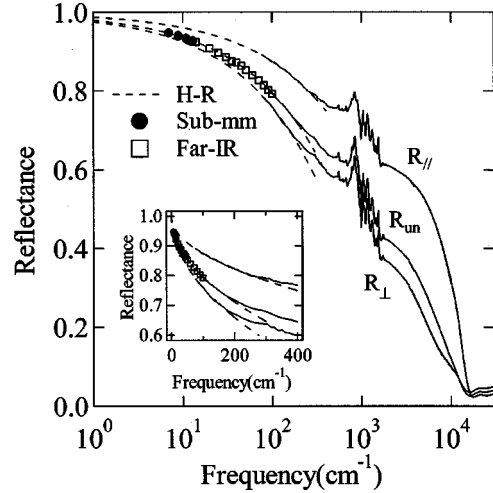


FIG. 1. Reflectance spectra, $R(\omega)$, of stretch-oriented PPy-PF₆ measured at 300 K with polarization parallel and perpendicular to the stretched direction, together with that of the nonoriented sample. The solid curves represent the measured $R(\omega)$. The dotted lines at the lowest frequencies indicate the extrapolation by the Hagen-Rubens (H-R) approximation. For the nonoriented sample, the H-R approximation is in excellent agreement with low-frequency $R(\omega)$ data obtained with the submillimeter spectrometer (\bullet ; $8 \leq \omega \leq 13 \text{ cm}^{-1}$) and the far-IR interferometer (\square ; $15 \leq \omega \leq 100 \text{ cm}^{-1}$). The inset shows $R(\omega)$ below 400 cm^{-1} on a linear scale; the Hagen-Rubens curves (dotted lines) are in excellent agreement with the measured $R(\omega)$ for $\omega < 250 \text{ cm}^{-1}$.

nonoriented sample with a pronounced additional feature near $1.1 \times 10^4 \text{ cm}^{-1}$.

For simple metals, the far-infrared reflectance can be approximated by the Hagen-Rubens (H-R) relation

$$R_{\text{H-R}}(\omega) \cong 1 - (2\omega/\pi\sigma_0)^{1/2} \quad (1)$$

for $\omega \ll \sigma_0$, where σ_0 is the static (dc) conductivity.²⁴ Thus, applicability of the H-R relation implies classical metallic behavior with $\sigma(\omega) = \sigma_0$ at low frequencies.²⁵ The data (see Figs. 1 and 2) indicate that for the parallel direction the H-R relation provides an excellent fit to $R(\omega)$ in the far IR [$\omega \leq 250 \text{ cm}^{-1}$ ($\approx 0.47 \times 10^4 \text{ sec}^{-1}$)]. Moreover, the condition $\omega \ll \sigma_0$ ($\approx 850 \text{ S/cm} \approx 7.7 \times 10^4 \text{ sec}^{-1}$) is well satisfied in this frequency range, and the σ_0 values obtained from the fits to Eq. (1) are in agreement with the measured dc conductivity, σ_{dc} (300 K). For the nonoriented sample, the extreme far-IR measurements precisely follow the H-R fit and overlap beautifully with the IR data ($\omega \geq 50 \text{ cm}^{-1}$), confirming the accuracy and validity of the H-R extrapolation. The excellent fits and the agreement between σ_0 and σ_{dc} (300 K) imply a weak ω dependence in the optical conductivity, $\sigma(\omega)$, for $\omega \leq 250 \text{ cm}^{-1}$.

Figure 2 displays $\sigma(\omega)$ as obtained from K-K analysis of $R(\omega)$ with appropriate extrapolation beyond the measurement range. At low frequencies, the H-R relation was used to extrapolate to $\omega \rightarrow 0$, as justified above. The $\sigma(\omega)$ data obtained from the oriented sample are consistent with the dc transport results. For the parallel direction, $\sigma(\omega)$ exhibits significantly enhanced intraband response throughout the IR as

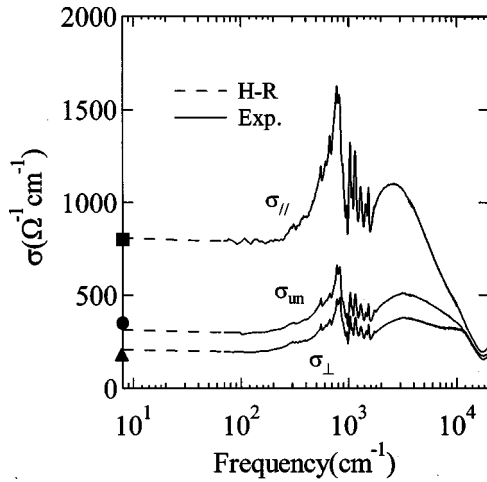


FIG. 2. Optical conductivity $\sigma(\omega)$ of PPy-PF₆ parallel and perpendicular to the stretched direction together with that of the non-oriented sample. Note the 1:1 correspondence between the dc conductivity (σ_{dc}), shown as the symbols, and $\sigma(\omega \rightarrow 0)$, as obtained from the K-K analysis with extrapolation to $\omega \rightarrow 0$ by the Hagen-Rubens approximation (dotted lines).

compared with that of the as-grown sample. Note, however, that the tensile-drawing (chain orientation) does not alter the essential physics of the samples. The decrease in $\sigma(\omega)$ below 2500 cm^{-1} (ignoring the phonon contributions near 1000 cm^{-1}), which has been attributed to disorder-induced localization in previous publications on nonoriented samples,^{5,6} is clearly observed in the oriented sample with no change in the peak position.

For both the parallel and perpendicular polarization directions, $\sigma(\omega)$ as obtained from the K-K analysis of $R(\omega)$ accurately approaches the measured σ_{dc} (300 K) value for frequencies below $\omega \sim 250 \text{ cm}^{-1}$. Indeed, such a weak ω dependence for $\omega \leq 250 \text{ cm}^{-1}$ is expected from the excellent fit of $R(\omega)$ by the H-R formula in this frequency range.

Chain orientation has a strong influence on the spectral dependence of $\varepsilon(\omega)$ as shown in Fig. 3. PPy-PF₆ is a disordered metal close to the M-I transition with $\omega_p \tau \sim 1$, where ω_p is the plasma frequency and τ is the scattering time. On the metallic side of the M-I transition where $\omega_p \tau > 1$, $\varepsilon(\omega)$ is expected to cross zero at the screened plasma frequency, $\Omega_p = \omega_p / (\varepsilon_\infty)^{1/2}$, where ε_∞ is the high-energy contribution to the dielectric constant. This is indeed the case for the parallel direction in the oriented sample; $\varepsilon(\omega)$ crosses zero at $1.3 \times 10^4 \text{ cm}^{-1}$ (1.6 eV) and goes to negative values in the near IR.

The importance of disorder is demonstrated by theoretical analysis using the “localization-modified Drude model,”^{4,5} as shown in Fig. 4. The fits to the data yield $\omega_p \approx 2.3 \text{ eV}$ (thus, $\Omega_p \approx 1.6 \text{ eV}$ with $\varepsilon_\infty \approx 2$), $\tau \approx 1.2 \times 10^{-15} \text{ sec}$, and $k_F \ell \approx 1.3$ for parallel polarization, where k_F is the Fermi wave number and ℓ is the mean free path. Using these values, we obtain $\omega_p \tau \approx 4.1 > 1$. However, in contrast to simple Drude behavior, weak localization causes $\varepsilon_1(\omega)$ to cross zero again at $\sim 2000 \text{ cm}^{-1}$ and remain positive down to $\sim 50 \text{ cm}^{-1}$ in the parallel direction for the partially oriented sample. The general agreement with the LMD model implies

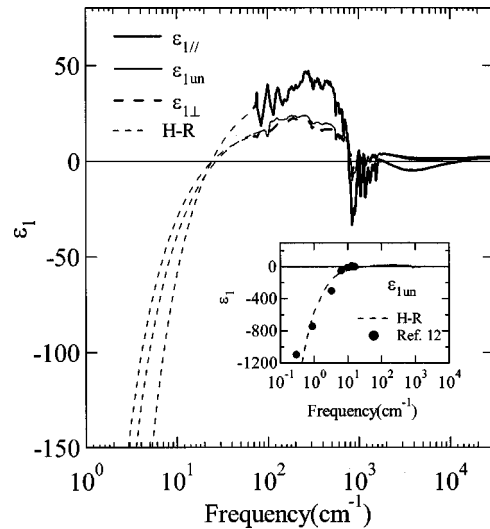


FIG. 3. Real part of the dielectric function $\varepsilon_1(\omega)$ of PPy-PF₆ parallel and perpendicular to the orientation direction together with that of the nonoriented sample. The inset compares $\varepsilon_1(\omega)$ of the nonoriented sample and data obtained from Ref. 12.

that in contrast to the inhomogeneous metallic island model, the disorder is “weak” in the context of disorder theory.

The corresponding fit of the LMD model to the data from the as-grown sample yields $\omega_p \approx 2.0 \text{ eV}$, $\tau \approx 0.7 \times 10^{-15} \text{ sec}$ ($\omega_p \tau \approx 2.1$), and $k_F \ell \approx 1.3$. The lower value for ω_p (2.0 vs 2.3 eV in the direction parallel in the oriented sample) is consistent with the $R(\omega)$ data shown in Fig. 1 and evidently arises from contributions to the oscillator strength polarized perpendicular to the metallic chains. For the nonoriented sample, $\omega_p \tau > 1$, which is sufficient to give a minimum in $R(\omega)$ but not quite large enough to bring $\varepsilon(\omega)$ down to zero. Note that $k_F \ell$, the order parameter in localization theory,²⁶ is the same ($k_F \ell \approx 1.3$) for the as-grown and oriented samples, implying that disorder is not significantly reduced by tensile drawing.

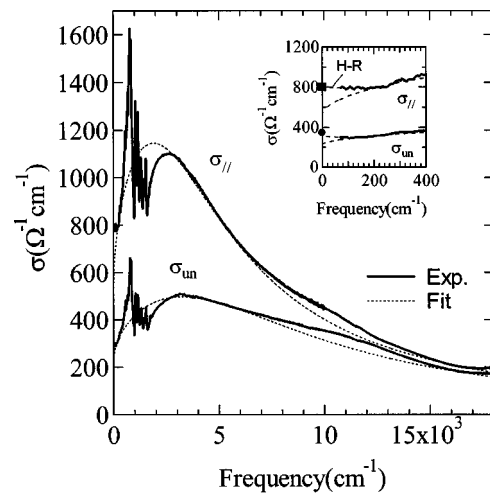


FIG. 4. Theoretical fits to the measured $\sigma(\omega)$ using the LMD model as explained in the text. The inset shows the low-frequency part with an expanded scale.

The positive $\varepsilon(\omega)$ in the far IR for $\omega > 50 \text{ cm}^{-1}$ is consistent with our previous observations^{5,6} and also with independent IR measurements⁷⁻⁹ carried out with high photometric accuracy. Since we have confidence in the accuracy of the low-frequency extrapolations (see Figs. 1 and 2), we can use the $\sigma(\omega)$ data to obtain $\varepsilon(\omega)$ as ω approaches zero; $\sigma(\omega)$ and $\varepsilon(\omega)$ must be K-K consistent. The results, shown in Fig. 3, indicate a second zero crossing to $\varepsilon_1(\omega) < 0$ at $\omega \approx 20 \text{ cm}^{-1}$. As shown in the inset of Fig. 3, the functional dependence of $\varepsilon(\omega)$ for $\omega < 20 \text{ cm}^{-1}$ is in excellent agreement with the terahertz measurements of Marten *et al.*^{12,13} The negative values for ε are also in agreement with the earlier microwave results.^{10,11}

Note that all the $\varepsilon(\omega)$ curves cross zero at the same frequency, regardless of chain orientation. Earlier studies^{14,15} reported a zero crossing around 250 cm^{-1} , one order-of-magnitude larger than at $\omega \approx 20 \text{ cm}^{-1}$, as shown in Fig. 3. The second zero crossing was attributed to a second plasma resonance associated with a low density of delocalized carriers with a remarkably long scattering time ($\tau \sim 10^{-11} \text{ s}$). However, the spectral dependence of $\sigma(\omega)$ at low frequencies provides insight into the origin of the negative $\varepsilon(\omega)$. The dielectric function will always cross zero to negative values in any sample where $\sigma(\omega)$ is constant at low frequencies and where the Hagen-Rubens expression provides an accurate fit to $R(\omega)$. The constant $\sigma(\omega)$ implies oscillator strength from the intraband transitions at low frequencies, as demonstrated in the deviation from the LMD model below $\sim 250 \text{ cm}^{-1}$ shown in the inset of Fig. 4. Thus, $\sigma(\omega) = \sigma_0$ implies a crossover in the charge dynamics in this frequency range. For $\omega > 250 \text{ cm}^{-1}$, the results are characteristic of a quasi-one-dimensional “metal” in which disorder-induced localization dominates the frequency dependence of $\sigma(\omega)$ and $\varepsilon(\omega)$. Below approximately 250 cm^{-1} , the charge dynamics

are characteristic of an anisotropic three-dimensional metal. Thus, the data imply a dimensionality-induced crossover in the metal physics of conducting polymers close to, but on the metallic side of, the M-I transition.

IV. SUMMARY AND CONCLUSION

In summary, polarized reflectance measurements on high-quality oriented films of metallic PPy-PF₆ demonstrate that the optical conductivity $\sigma(\omega)$ becomes frequency independent below approximately 250 cm^{-1} and that there is a zero crossing in the dielectric function $\varepsilon(\omega)$ to negative values below 20 cm^{-1} . Since $\sigma(\omega)$ extrapolates to the dc value and since $\varepsilon(\omega)$ is in excellent agreement with the data obtained from terahertz and microwave measurements, the controversy in the dielectric response of the metal physics of conducting polymers is finally resolved. The photon energy at which the crossover occurs is comparable to the magnitude of the interchain transfer integral ($t_{\perp} \approx 0.01-0.1 \text{ eV}$) in conducting polymers,²⁷ consistent with a crossover from one- ($\hbar\omega > t_{\perp}$) to three-dimensional ($\hbar\omega < t_{\perp}$) charge dynamics. In general, this dimensionality-induced crossover in the transport properties is well known in the physics of quasi-one-dimensional conductors with finite interchain coupling.²⁸

ACKNOWLEDGMENT

We thank Professor G. Grüner for providing submillimeter spectroscopic data and Professor Y. H. Kim for supplementing the high-precision far IR. K. L. acknowledges the financial support from the Basic Research Program of the Korea Science and Engineering Foundation under Grant No. R01-2000-000-00013-0. Work at UCSB was carried out under support from the National Science Foundation under Grant No. NSF-DMR-0099843.

¹See, for example, A. J. Heeger, *Rev. Mod. Phys.* **73**, 681 (2001).

²R. Menon, C. O. Yoon, D. Moses, and A. J. Heeger, in *Handbook of Conducting Polymers*, 2nd ed., edited by T. A. Skotheim, R. L. Elsenbaumer, and J. R. Reynolds (Marcel Dekker, New York, 1998).

³R. S. Kohlman, J. Joo, and A. J. Epstein, in *Physical Properties of Polymers Handbook*, edited by J. E. Mark (AIP, New York, 1996).

⁴R. Kiebooms, R. Menon and K. Lee, in *Handbook of Advanced Electronic and Photonic Materials and Devices*, edited by H. S. Nalwa (Academic, San Diego, 2001), Vol. 8.

⁵K. Lee, R. Menon, C. O. Yoon, and A. J. Heeger, *Phys. Rev. B* **52**, 4779 (1995).

⁶K. Lee, E. K. Miller, A. N. Aleshin, R. Menon, A. J. Heeger, J. H. Kim, C. O. Yoon, and H. Lee, *Adv. Mater. (Weinheim, Ger.)* **10**, 456 (1998).

⁷B. Chapman, R. G. Buckley, N. T. Kemp, A. B. Kaiser, D. Beaglehole, and H. J. Trodahl, *Phys. Rev. B* **60**, 13 479 (1999).

⁸N. Petit, F. Gervais, P. Buvat, P. Hourquebie, and P. Topart, *Eur. Phys. J. B* **12**, 367 (1999).

⁹G. Tzamalidis, N. A. Zaidi, C. C. Homes, and A. P. Monkman,

Phys. Rev. B **66**, 085202 (2002).

¹⁰J. Joo, Z. Oblakowski, G. Du, J. P. Pouget, E. J. Oh, J. M. Weisinger, Y. G. Min, A. G. MacDiarmid, and A. J. Epstein, *Phys. Rev. B* **49**, 2977 (1994).

¹¹R. S. Kohlman, J. Joo, Y. Z. Wang, J. P. Pouget, H. Kaneko, T. Ishiguro, and A. J. Epstein, *Phys. Rev. Lett.* **74**, 773 (1995).

¹²H. C. F. Martens, J. A. Reedijk, H. B. Brom, D. M. de Leeuw, and R. Menon, *Phys. Rev. B* **63**, 073203 (2001).

¹³H. C. F. Martens, H. B. Brom, and R. Menon, *Phys. Rev. B* **64**, 201102 (2001).

¹⁴R. Kohlman, J. Joo, Y. G. Min, A. G. MacDiarmid, and A. J. Epstein, *Phys. Rev. Lett.* **77**, 2766 (1996).

¹⁵R. S. Kohlman, A. Zibold, D. B. Tanner, G. G. Ihas, T. Ishiguro, Y. G. Min, A. G. MacDiarmid, and A. J. Epstein, *Phys. Rev. Lett.* **78**, 3915 (1997).

¹⁶Y. Nogami, J.-P. Pouget, and T. Ishiguro, *Synth. Met.* **62**, 257 (1994).

¹⁷J. P. Pouget, Z. Oblakowski, Y. Nogami, P. A. Albouy, M. Laridjani, E. J. Oh, Y. Min, A. G. MacDiarmid, J. Tsukamoto, T. Ishiguro, and A. J. Epstein, *Synth. Met.* **65**, 131 (1994).

¹⁸N. F. Mott, *Metal-Insulator Transitions* (Taylor & Francis, London, 1990).

- ¹⁹T. G. Castner, in *Hopping Transport in Solids*, edited by M. Polak and B. I. Shklovskii (North-Holland, Amsterdam, 1991).
- ²⁰R. Singh, A. K. Narula, R. P. Tandon, A. Mansingh, and S. Chandra, *J. Appl. Phys.* **80**, 985 (1996).
- ²¹A. N. Papathanassiou, J. Grammatikakis, S. Sakkopoulos, E. Vitoratos, and E. Dalas, *J. Phys. Chem. Solids* **63**, 1771 (2002); A. N. Papathanassiou, I. Sakellis, J. Grammatikakis, S. Sakkopoulos, E. Vitoratos, and E. Dalas, *Solid State Commun.* **125**, 95 (2003).
- ²²C. O. Yoon, H. K. Sung, J. H. Kim, E. Barsoukov, J. H. Kim, and H. Lee, *Synth. Met.* **99**, 201 (1999).
- ²³See, e.g., F. Wooten, *Optical Properties of Solids* (Academic, New York, 1972).
- ²⁴E. Hagen and H. Rubens, *Ann. Phys. (N.Y.)* **11**, 873 (1903).
- ²⁵C. Kittel, *Introduction to Solid State Physics* (Wiley, New York, 1996).
- ²⁶P. A. Lee and T. V. Ramakrishnan, *Rev. Mod. Phys.* **57**, 287 (1985).
- ²⁷K. Lee and A. J. Heeger, *Synth. Met.* **128**, 279 (2002).
- ²⁸See, for example, V. Vescoli, L. Degiorgi, W. Henderson, G. Grüner, K. P. Starkey, and L. K. Montgomery, *Science* **281**, 1181 (1998).